Supplemental Information

Supplemental Figures and Legends

Figure S1 and Table S1, related to Figure 1. (A) Schematic model for fifteen T-Rex and cpYFP chimeras. **(B)** Fluorescence response of fifteen chimeras in the presence of 18 μM NADH and 18 μM NAD^+. **(C and D)** Truncation mutants of F189/L190 with **(C)** or without **(D)** the DNA-binding domain of T-Rex and their fluorescence response towards 18 μM NADH and its analogs. **(E and F)** Emission spectra of purified SoNar in the control condition (black), and after addition of 20 μM NAD^+ (green) or 20 μM NADH (orange), normalized to the peak intensity in the control condition. Excitation was fixed at 420 nm **(E)** and 490 nm **(F)**, respectively. **(G)** Fluorescence intensities of SoNar with excitation at 420 nm or 485 nm in the presence of different concentrations of NADH and NAD^+, and emission at 528 nm. Data normalized to the initial value. **(H)** SoNar fluorescence plotted against the NAD^+/NADH ratio in the presence of $NADP^+$ (20 μM) and NADPH (20 μM). **(I)** SoNar fluorescence plotted against the NAD^+/NADH ratio in the presence of ATP (5 mM) and ADP (5 mM). **(J)** SoNar fluorescence plotted against the NAD^+/NADH ratio at the indicated ATP: ADP ratios; the total adenine nucleotide concentration was 5 mM. **(K)** Ratio of SoNar fluorescence excited at 420 nm and 485 nm at the indicated pH plotted against the NAD^+/NADH ratio. **(L)** Fluorescence intensities of SoNar and cpYFP with excitation at 420 nm or 485 nm, and emission at 528 nm. Data normalized to the fluorescence at pH 7.4. **(M)** pH-dependency of the excitation ratio 420/485 nm of SoNar and cpYFP. For panel **Figures S1H**-**S1K**, the total nicotinamide adenine dinucleotide concentration was 400 μM. Fluorescence ratios were normalized to the value in the presence of NADH (400 μM) at pH 7.4. For panel **Figures S1G**-**S1M**, error bars represent SEM.

Figure S2, related to Figure 2. (A) Comparison of the fluorescence intensity of

different genetically encoded fluorescent sensors in H1299 cells. **(B)** Dose-dependent response of SoNar, cpYFP, Frex, and Peredox fluorescence to different concentrations of pyruvate in H1299 cells. For Peredox (blue), cells were excited at 400 nm and treated for 30 min. For Frex (black), cells were excited at 485 nm and measured immediately after pyruvate addition. For SoNar and cpYFP, fluorescence was excited at 420 nm and 485 nm and emission measured at 528 nm immediately after pyruvate addition. Data were normalized to samples without pyruvate incubation. **(C)** Time course of responses of Peredox fluorescence excited at 400 nm in H1299 cells treated with different concentrations of exogenous pyruvate. **(D)** Dose-dependent response of SoNar, cpYFP, and Peredox fluorescence in H1299 cells to different concentrations of lactate or oxamate. Fluorescence response of SoNar and cpYFP with excitation at 420 nm and 485 nm. Fluorescence response of Peredox with excitation at 400 nm. Cells were treated for 30 min. **(E)** Spatiotemporally resolved changes in the ratiometric fluorescence of SoNar or cpYFP in sequential frames (left to right, 30 s per frame) in response to 5 mM oxamate in H1299 cells. Images were pseudocolored with the ratio of fluorescence excited at 425 nm and 482 nm. Scale bar, 10 μm. **(F)** The ratio of corrected SoNar fluorescence by normalization with cpYFP excited at 420 nm and 485 nm in various cells and measured *in vitro* with a fluorescence plate reader in the presence or absence of 400 μM NAD^+ or 400 μM NADH. **(G)** Responses of SoNar and Peredox to different NAD^+/NADH ratios. For SoNar, the total nicotinamide adenine dinucleotide concentration was 400 μM. Fluorescence ratios were normalized to the value in the presence of NAD^+ (400 μM), at pH 7.4. For Peredox, fluorescence ratios were normalized to the control condition in the absence of pyridine nucleotides at pH 7.2, with 230 μM NAD^+ (data redrawn from previous work) (Hung et al., 2011). **(H)** Dose-dependent response of cytosolic SoNar and cpYFP fluorescence to different concentrations of 3-BrPA in H1299 cells. The dark red line represents the fluorescence response of SoNar corrected for pH effects. Cells were measured immediately after 3-BrPA addition. Data are normalized to samples without 3-BrPA incubation. **(I)** Kinetics of fluorescence response of the cytosolic SoNar and cpYFP in glucose-starved cells after 5 mM glucose supplementation in

H1299 cells. **(J)** Dose-dependent fluorescence response of cytosolic SoNar and cpYFP to different concentrations of glucose in H1299 and HEK293 cells. Cells were treated for 10 min. **(K)** The central role NAD^+/NADH playing in relevant metabolic pathways. The NADH molecules produced from glucose, fatty acid, and amino acid catabolism were oxidized to generate ATP by the mitochondrial respiratory chain. Glycolysis-derived NADH is transferred to mitochondria through the NADH shuttle system. Error bars represent SEM.

Figure S3 and Table S2, related to Figure 3. (A) Relative proportion of compounds that markedly decreased or increased the intracellular NAD^+/NADH ratio across different chemical libraries. **(B)** Top 78 hit compounds that decreased NAD^+/NADH ratio in H1299 cells, identified by high-throughput screening. **(C)** Effects of these hit compounds on H1299 cell viability. **(D and E)** Effects of compounds that increase the NAD^+/NADH ratio on SoNar **(D)** and cpYFP **(E)** fluorescence in H1299 cells. Data derived from microscopy data of **Figures 3D and 3E** and normalized to untreated cells. Error bars represent SD.

Figure S4 and Table S3, related to Figure 4. (A) Plasma drug concentration-time profile of KP372-1 in BALB/c mice following intravenous (IV, 1 mg/kg) and oral administration (PO, 5 mg/kg). Error bars indicate SEM with N=4 per time point. **(B)** Quantification of SoNar and cpYFP fluorescence in H1299 xenografts before and after tail vein injection of KP372-1. Data derived from Figures 4A and 4B. Error bars represent SD. **(C)** Mean weight of H1299 xenografts dissected at day 33 in mice treated orally daily with the indicated doses of KP372-1. Error bars indicate SEM. **(D)** KP372-1 decreases proliferation (Ki67 staining) and increases apoptosis (Caspase-3 and TUNEL staining) in subcutaneous H1299 tumors harvested from intact mice. Percentage of Ki67 or caspase-3 positive cells were counted in sections from two xenografts for each treatment. At least 1000 cells per xenograft were counted, n = 2 tumors. Representative slides with staining are shown. Error bars indicate SEM. **(E-I)** KP372-1-induced H1299 cell apoptosis was detected by annexin V–FITC/PI staining

(E), caspase-3 activity **(F)**, cleaved caspase-3 **(G)**, mitochondrial membrane permeabilization **(H),** and enhanced Bax localization in mitochondria **(I)**. For annexin V–FITC/PI staining, H1299 cells were treated with 0.5 μM KP372-1 for 24 h. For caspase-3 activity assay, H1299 cells were treated with 0.5 μM KP372-1 for 8 h. For western assay of caspase-3 and cleaved caspase-3, H1299 cells were treated with different concentrations of KP372-1 for 2 h. For immunofluorescence detection of Bax, H1299 cells were treated with 0.5 μM KP372-1 for 2 h. Error bars indicate SEM. **(J-M)** KP372-1-induced A549 cell apoptosis was detected by annexin V–FITC/PI staining **(J)**, cleaved caspase-3 **(K)**, mitochondrial membrane permeabilization **(L)** and enhanced Bax localization on mitochondria **(M)**. For annexin V–FITC/PI staining, A549 cells were treated with different concentrations of KP372-1 for 15 h. For western assay of caspase-3 and cleaved caspase-3, A549 cells were treated with different concentrations of KP372-1 for 2 h. For immunofluorescence detection of Bax, A549 cells were treated with different concentrations of KP372-1 for 2 h. Error bars indicate SEM. **(N)** Changes in the body weight of mice treated orally daily with indicated doses of KP372-1, n=8 in each group. Error bars indicate SEM. **(O)** KP372-1-treated mice did not have signs of liver (ALT and AST), kidney (creatinine), or blood (hemoglobin) toxicity, n=8 in each group. Error bars indicate SEM. **(P)** KP372-1 did not induce apoptosis in normal tissues (heart, liver, lung and kidney).

Figure S5 and Table S4, related to Figure 5. (A) Metabolite profiles of KP372-1-treated cells shown as heat maps. Metabolites that increased in concentration are shown in red whereas metabolites that decreased in concentration are shown in green. H1299 cells were treated with 5 μM KP372-1 for 5 min and 60 min, respectively. **(B-D)** Effect of KP372-1 on levels of intracellular pyruvate **(B)**, lactate **(C)**, and NAD^+/NADH ratio **(D)** in H1299 cells monitored using fluorescence-based assay kits for pyruvate or lactate. NAD^+/NADH ratio was calculated according to the equilibrium constants of lactate dehydrogenase. **(E and F)** Effect of KP372-1 on extracellular pyruvate **(E)** and lactate **(F)** production in H1299 cells (n=3 in each group). ***$p < 0.001$. **$0.001 < p < 0.01$. NS, not significant. **(G)**

KP372-1 increased intracellular $NADP^+$ levels. Data obtained by metabolomic analysis (n=5 in each group). ***p < 0.001. **(H-K)** Kinetics of fluorescence responses of SoNar **(H)**, Hyper **(I)**, roGFP1 **(J)**, and cpYFP **(K)** sensors expressed in H1299 cells to 0.5 μM KP372-1 and different oxidants. **(L)** Time-lapse fluorescence imaging of H1299 cells expressing roGFP1 (left to right, 1 min per frame) in response to 0.5 μM KP372-1. Ratios of fluorescence excited at 407 nm and 482 nm were used to pseudocolor the images. Scale bar, 10 μm. **(M)** Fluorescence imaging of H1299 cells expressing Hyper or cpYFP before and 30 s after treatment with 0.5 μM KP372-1. Images were pseudocolored with the ratio of fluorescence excited at 425 nm and 482 nm. Scale bar, 10 μm. **(N)** Kinetics of fluorescence responses of H1299 cells expressing SoNar, Hyper, and roGFP1 to 0.1 μM KP372-1. (**O and P**) KP372-1- induced cell death was largely blocked by catalase overexpression, N-acetylcysteine, or Tiron in H1299 cells. H1299 cells were pretreated for 0.5 h with N-acetylcysteine, a general antioxidant, or Tiron, a cell permeable superoxide scavenger. Error bars represent SEM.

Figure S6, related to Figure 6. **(A)** Overexpression of NQO1, but not other NAD(P)H oxidases, increases KP372-1-induced NADH oxidation, H_2O_2 production, thiol oxidation, and cell death in H1299 cells. **(B)** The NQO1 inhibitor dicoumarol, but not other pharmacologic inhibitors of ROS-generating enzymes, decrease KP372-1-induced NADH oxidation, H_2O_2 production, and thiol oxidation in A549 cells. **(A)** and **(B)** are the bar plots of same data set from Figures 6A and 6B. **(C)** Effects of NQO1 overexpression on KP372-1-induced NADH oxidation measured by SoNar fluorescence, H_2O_2 production measured by Hyper fluorescence**,** thiol oxidation measured by roGFP1 fluorescence, and cell death in H1299 cells. **(D)** Effects of dicumarol on KP372-1-induced NADH oxidation measured by SoNar fluorescence, H_2O_2 production measured by Hyper fluorescence**,** thiol oxidation measured by roGFP1 fluorescence, and cell death in A549 cells. For C-D, after cells were treated with KP372-1, SoNar fluorescence was measured immediately, while Hyper and roGFP1 fluorescence were measured after 10 min. A549 cells were treated with various KP372-1 doses with or without 50 μM dicumarol (Dic, 30 min). **(E)** Effect of

NQO1 overexpression and KP372-1 treatment on levels of intracellular pyruvate (left), lactate (middle), and NAD^+/NADH ratio (right) in H1299, measured using fluorescence-based assays for pyruvate or lactate. NAD^+/NADH ratio was calculated according to the equilibrium constants of lactate dehydrogenase. **(F)** Overexpression of several NAD(P)H oxidases in H1299 cells. Proteins were expressed with Flag tags and assessed by Western blot. **(G)** Effect of NQO1 inhibition and KP372-1 treatment on levels of intracellular pyruvate (left), lactate (middle), and NAD^+/NADH ratio (right) in A549 cells, measured using fluorescence-based assays for pyruvate or lactate. NAD^+/NADH ratio was calculated according to the equilibrium constants of lactate dehydrogenase. **(H)** Western blotting of endogenous NQO1 expressed in A549, H1299 and H596 NSCLC cells. **(I)** Sequences of NQO1 locus in A549 cells. Partial coding sequences of targeted genes in the genome containing the CRISPR/Cas9 sgNQO1-1 or sgNQO1-2 binding region (red) and sequencing analysis of the mutated alleles from monoclone cell lines. 12 TA clones of the PCR products were analyzed by DNA sequencing. The PAM sequences are underlined and highlighted in green; the mutations in blue, lower case; deletions (-), insertions (+). **(J)** Knockout of NQO1 decreased β-lapachone-induced NADH oxidation measured by SoNar fluorescence, H_2O_2 production measured by Hyper fluorescence**,** thiol oxidation measured by roGFP1 fluorescence, and cell death in A549 cells. After cells were treated with β-lapachone, SoNar fluorescence was measured immediately, while Hyper and roGFP1 fluorescence were measured after 10 min. **(K)** The effect of NQO1 inhibitor dicoumarol on β-lapachone cytoxicity to different cancer cell lines. Cells were exposed to a 4-h pulse of β-lapachone either with or without 50 μM dicoumarol and then grown for 24 h. **(L-O)** Comparison of endogenous NQO1 levels (**L**), sensitivity to KP372-1 (**M**), total GSH levels (**N**), sensitivity to H_2O_2 (**O**) between 5 KEAP1 wild-type cell lines (H292, H1299, H23, H1703 and H358) and 4 KEAP1-inactive mutant cell lines (A549, H460, H838 and H2126). Endogenous NQO1 levels were assayed by western blotting. NQO1 levels are presented relative to the level in H1299. For testing the sensitivity of different cells to KP372-1, cells were seeded in 96 well plates and treated with different concentrations of KP372-1 for 48 h. Survival was assessed using

CCK-8 kit. For the sensitivity of different cells to H_2O_2 assay, cells were exposed to H_2O_2 for 4 h and counted after 24 h. **(P)** Sequences of NQO1 locus in H1299 cells. Partial coding sequences of targeted genes in the genome containing the CRISPR/Cas9 sgNQO1-3 binding region (red) and sequencing analysis of the mutated alleles from monoclone cell lines. Four TA clones of the PCR products were analyzed by DNA sequencing. The PAM sequences are underlined and highlighted in green; (-) indicates deletions. **(Q-T).** Effects of combinations of 1 μM Akt inhibitors (Akt-I-1, Akt-I-1,2, GSK690693, BML-257, Akt Inhibitor IV, Akt Inhibitor V, Akt Inhibitor VIII, Akt Inhibitor X, Akt Inhibitor XII) on intracellular redox homeostasis monitored by corrected SoNar fluorescence in A549 cells **(Q)** and in H1299 cells **(S)**, and roGFP1 fluorescence in A549 cells **(R)** and in H1299 cells **(T)**. **(U)** Time course of Akt phosphorylation in H1299 and A549 cells treated with 0.5 μM KP372-1. **(V)** NQO1-catalyzed NADPH oxidation in the presence of KP372-1 *in vitro*. NADPH level was monitored by its endogenous fluorescence. The concentration of KP372-1 is indicated adjacent to each curve. **(W)** NADH oxidation monitored by the fluorescence response of SoNar *in vitro*, in the presence or absence of 100 μM NADH, 0.5 μM KP372-1, and 1 μg/ml NQO1. **(X)** Hydrogen peroxide production by an Amplex red/ horseradish peroxidase-based fluorescence assay in an assay solution containing 10 μM NADH and KP372-1, in the presence or absence of 1 μg/ml NQO1, and/or 30 U/ml superoxide dismutase, and/or 900 U/ml catalase. **(Y)** NQO1 overexpression accelerated 0.5 μM KP372-1-mediated oxygen consumption in H1299 cells. Error bars represent SEM.

Figure S1

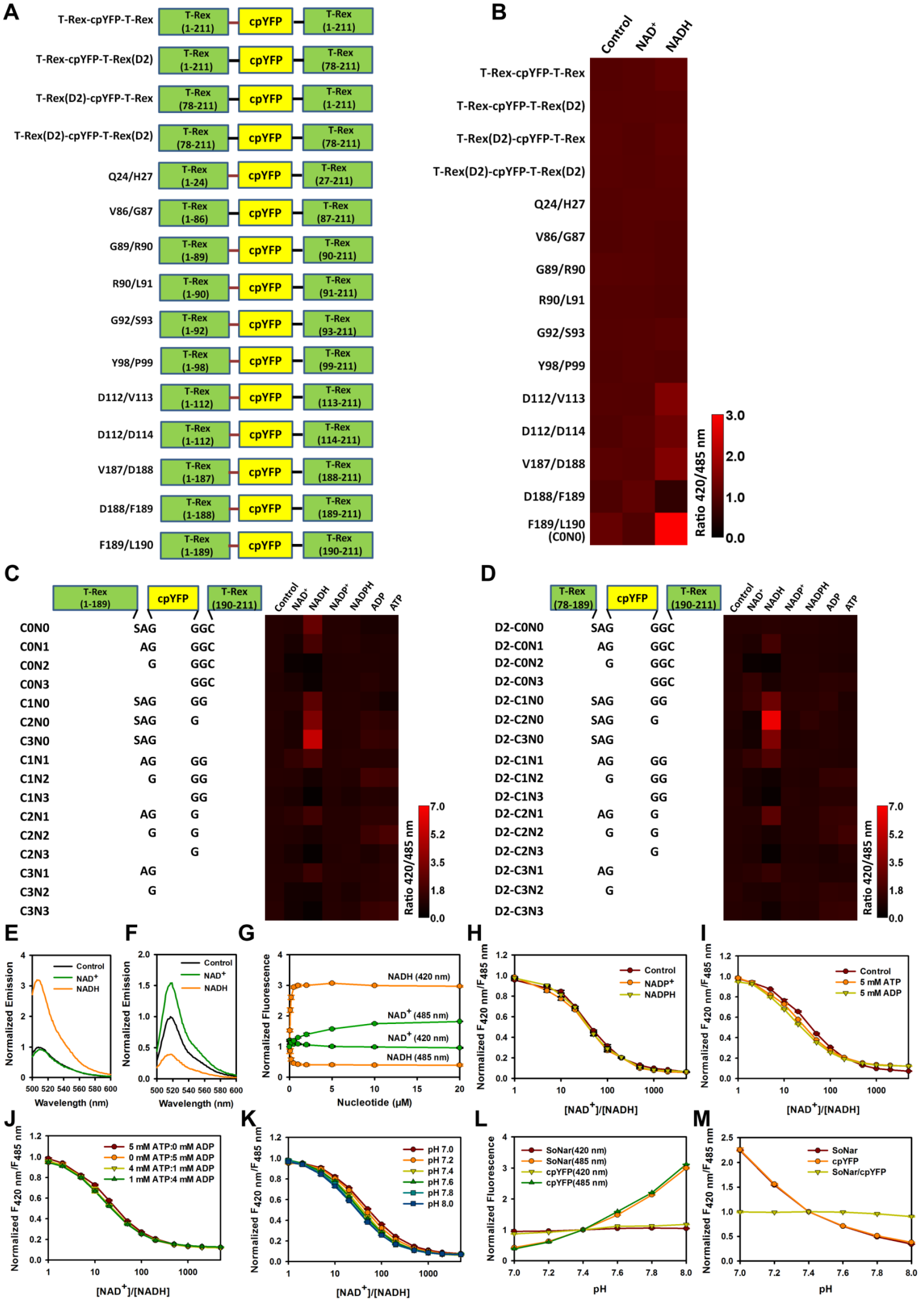
A
T-Rex-cpYFP-T-Rex
T-Rex-cpYFP-T-Rex(D2)
T-Rex(D2)-cpYFP-T-Rex
T-Rex(D2)-cpYFP-T-Rex(D2)
Q24/H27
V86/G87
G89/R90
R90/L91
G92/S93
Y98/P99
D112/V113
D112/D114
V187/D188
D188/F189
F189/L190
T-Rex (1-211)
T-Rex (78-211)
T-Rex (1-24)
T-Rex (27-211)
T-Rex (1-86)
T-Rex (87-211)
T-Rex (1-89)
T-Rex (90-211)
T-Rex (1-90)
T-Rex (91-211)
T-Rex (1-92)
T-Rex (93-211)
T-Rex (1-98)
T-Rex (99-211)
T-Rex (1-112)
T-Rex (113-211)
T-Rex (1-187)
T-Rex (188-211)
T-Rex (1-188)
T-Rex (189-211)
T-Rex (1-189)
T-Rex (190-211)
cpYFP
B
Control
NAD+
NADH
F189/L190 (C0N0)
Ratio 420/485 nm
3.0
2.0
1.0
0.0
C
T-Rex (1-189)
T-Rex (190-211)
C0N0
C0N1
C0N2
C0N3
C1N0
C2N0
C3N0
C1N1
C1N2
C1N3
C2N1
C2N2
C2N3
C3N1
C3N2
C3N3
SAG
AG
G
GGC
GG
NADP+
NADPH
ADP
ATP
7.0
5.2
3.5
1.8
0.0
D
T-Rex (78-189)
D2-C0N0
D2-C0N1
D2-C0N2
D2-C0N3
D2-C1N0
D2-C2N0
D2-C3N0
D2-C1N1
D2-C1N2
D2-C1N3
D2-C2N1
D2-C2N2
D2-C2N3
D2-C3N1
D2-C3N2
D2-C3N3
E
Normalized Emission
Wavelength (nm)
F
G
Normalized Fluorescence
NADH (420 nm)
NAD+ (485 nm)
NAD+ (420 nm)
NADH (485 nm)
Nucleotide (μM)
H
Normalized F420 nm/F485 nm
[NAD+]/[NADH]
I
5 mM ATP
5 mM ADP
J
5 mM ATP:0 mM ADP
0 mM ATP:5 mM ADP
4 mM ATP:1 mM ADP
1 mM ATP:4 mM ADP
K
pH 7.0
pH 7.2
pH 7.4
pH 7.6
pH 7.8
pH 8.0
L
SoNar(420 nm)
SoNar(485 nm)
cpYFP(420 nm)
cpYFP(485 nm)
pH
M
SoNar
cpYFP
SoNar/cpYFP

Figure S2

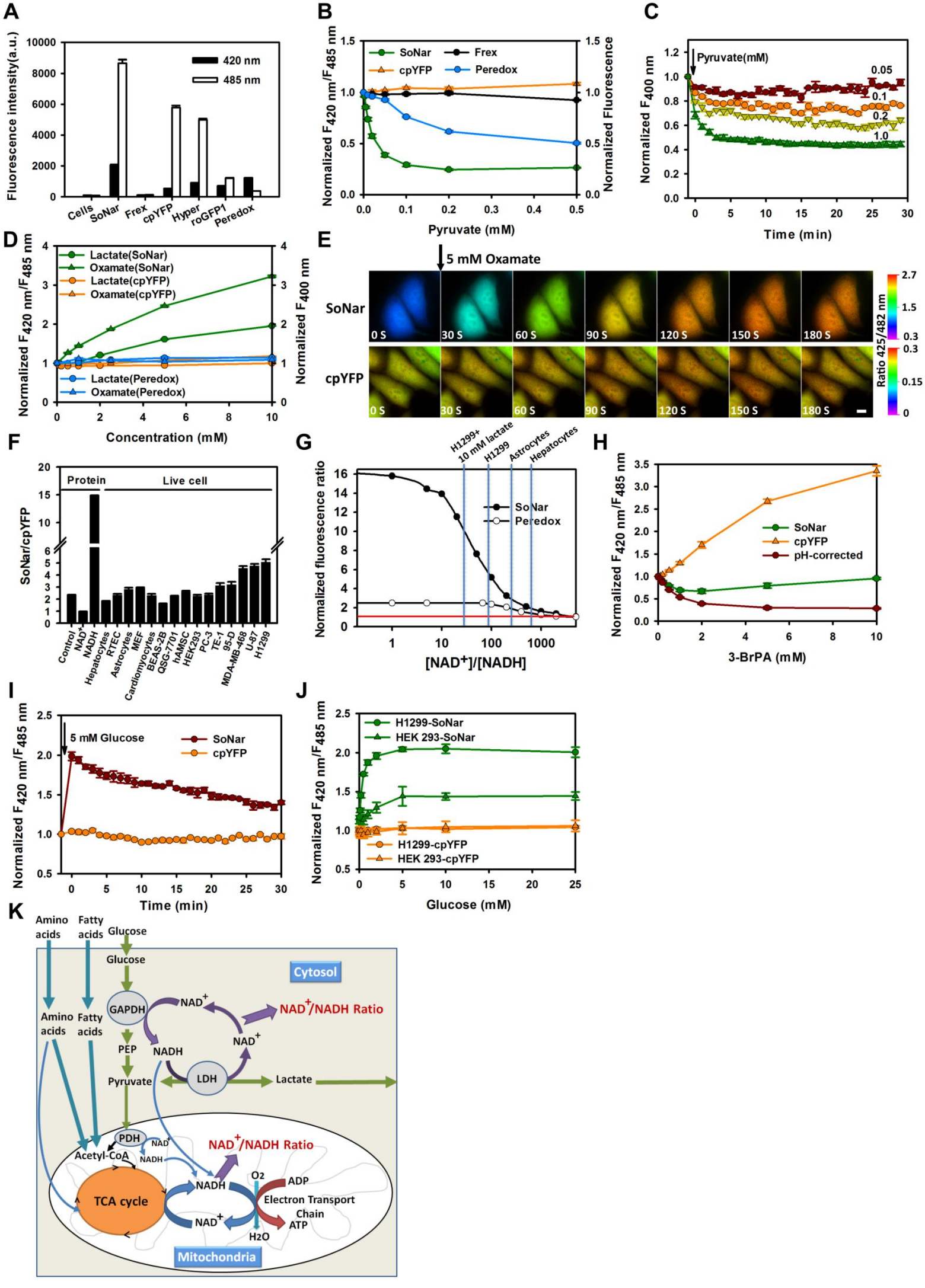
A
Fluorescence intensity(a.u.)
420 nm
485 nm
Cells
SoNar
Frex
cpYFP
Hyper
roGFP1
Peredox
B
Normalized F420 nm/F485 nm
Normalized Fluorescence
SoNar
Frex
cpYFP
Peredox
Pyruvate (mM)
C
Normalized F400 nm
Pyruvate(mM)
0.05
0.1
0.2
1.0
Time (min)
D
Normalized F420 nm/F485 nm
Normalized F400 nm
Lactate(SoNar)
Oxamate(SoNar)
Lactate(cpYFP)
Oxamate(cpYFP)
Lactate(Peredox)
Oxamate(Peredox)
Concentration (mM)
E
5 mM Oxamate
SoNar
cpYFP
0 S
30 S
60 S
90 S
120 S
150 S
180 S
Ratio 425/482 nm
F
SoNar/cpYFP
Protein
Live cell
Control
NAD+
NADH
Hepatocytes
RTEC
Astrocytes
MEF
Cardiomyocytes
BEAS-2B
QSG-7701
hAMSC
HEK293
PC-3
TE-1
95-D
MDA-MB-468
U-87
H1299
G
Normalized fluorescence ratio
H1299+ 10 mM lactate
H1299
Astrocytes
Hepatocytes
SoNar
Peredox
[NAD+]/[NADH]
H
Normalized F420 nm/F485 nm
SoNar
cpYFP
pH-corrected
3-BrPA (mM)
I
Normalized F420 nm/F485 nm
5 mM Glucose
SoNar
cpYFP
Time (min)
J
Normalized F420 nm/F485 nm
H1299-SoNar
HEK 293-SoNar
H1299-cpYFP
HEK 293-cpYFP
Glucose (mM)
K
Amino acids
Fatty acids
Glucose
Cytosol
GAPDH
NAD+
NAD+/NADH Ratio
PEP
NADH
Pyruvate
LDH
Lactate
PDH
Acetyl-CoA
TCA cycle
O2
ADP
Electron Transport Chain
ATP
H2O
Mitochondria

Figure S3

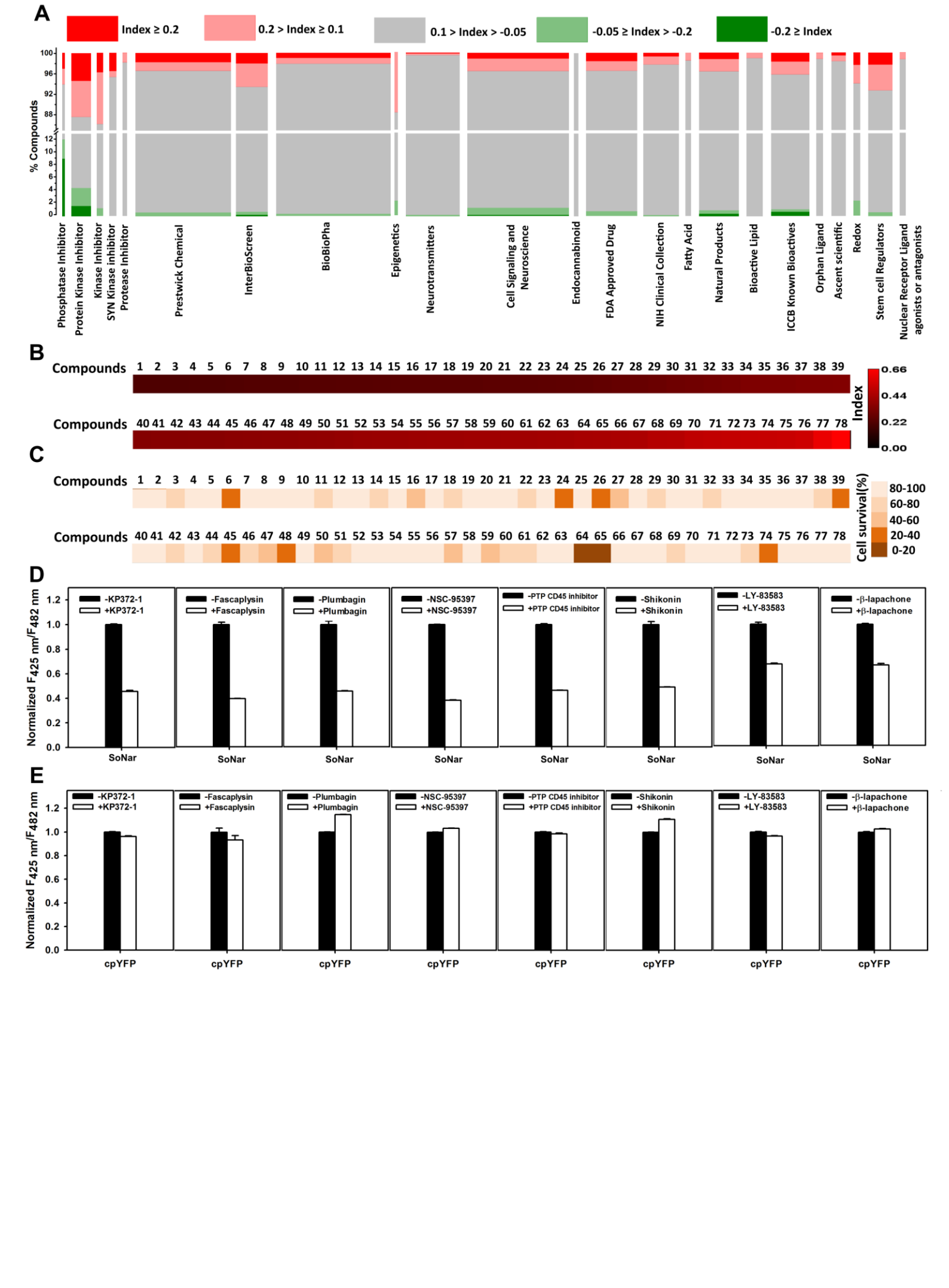
A
Index ≥ 0.2
0.2 > Index ≥ 0.1
0.1 > Index > -0.05
-0.05 ≥ Index > -0.2
-0.2 ≥ Index
% Compounds
Phosphatase Inhibitor
Protein Kinase Inhibitor
Kinase Inhibitor
SYN Kinase inhibitor
Protease Inhibitor
Prestwick Chemical
InterBioScreen
BioBioPha
Epigenetics
Neurotransmitters
Cell Signaling and Neuroscience
Endocannabinoid
FDA Approved Drug
NIH Clinical Collection
Fatty Acid
Natural Products
Bioactive Lipid
ICCB Known Bioactives
Orphan Ligand
Ascent scientific
Redox
Stem cell Regulators
Nuclear Receptor Ligand agonists or antagonists
B
Compounds
Index
C
Cell survival(%)
80-100
60-80
40-60
20-40
0-20
D
Normalized F425 nm/F482 nm
-KP372-1
+KP372-1
-Fascaplysin
+Fascaplysin
-Plumbagin
+Plumbagin
-NSC-95397
+NSC-95397
-PTP CD45 inhibitor
+PTP CD45 inhibitor
-Shikonin
+Shikonin
-LY-83583
+LY-83583
-β-lapachone
+β-lapachone
SoNar
E
cpYFP

Figure S4

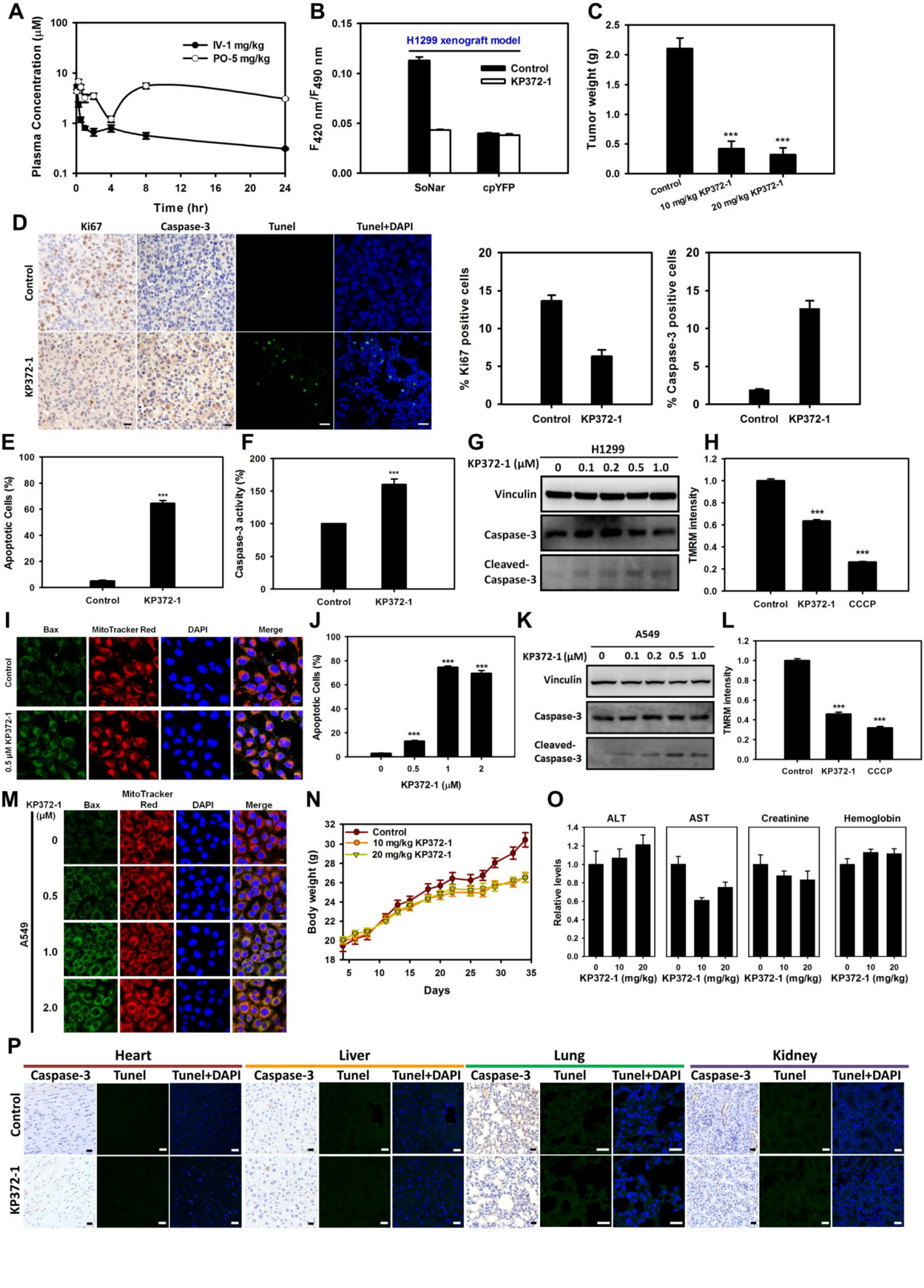
A
Plasma Concentration (μM)
IV-1 mg/kg
PO-5 mg/kg
Time (hr)
B
H1299 xenograft model
Control
KP372-1
F420 nm/F490 nm
SoNar
cpYFP
C
Tumor weight (g)
Control
10 mg/kg KP372-1
20 mg/kg KP372-1
D
Ki67
Caspase-3
Tunel
Tunel+DAPI
Control
KP372-1
% Ki67 positive cells
% Caspase-3 positive cells
E
Apoptotic Cells (%)
F
Caspase-3 activity (%)
G
H1299
KP372-1 (μM)
Vinculin
Caspase-3
Cleaved-Caspase-3
H
TMRM intensity
CCCP
I
Bax
MitoTracker Red
DAPI
Merge
0.5 μM KP372-1
J
Apoptotic Cells (%)
K
A549
L
M
MitoTracker Red
N
Body weight (g)
Days
O
ALT
AST
Creatinine
Hemoglobin
Relative levels
P
Heart
Liver
Lung
Kidney

Figure S5

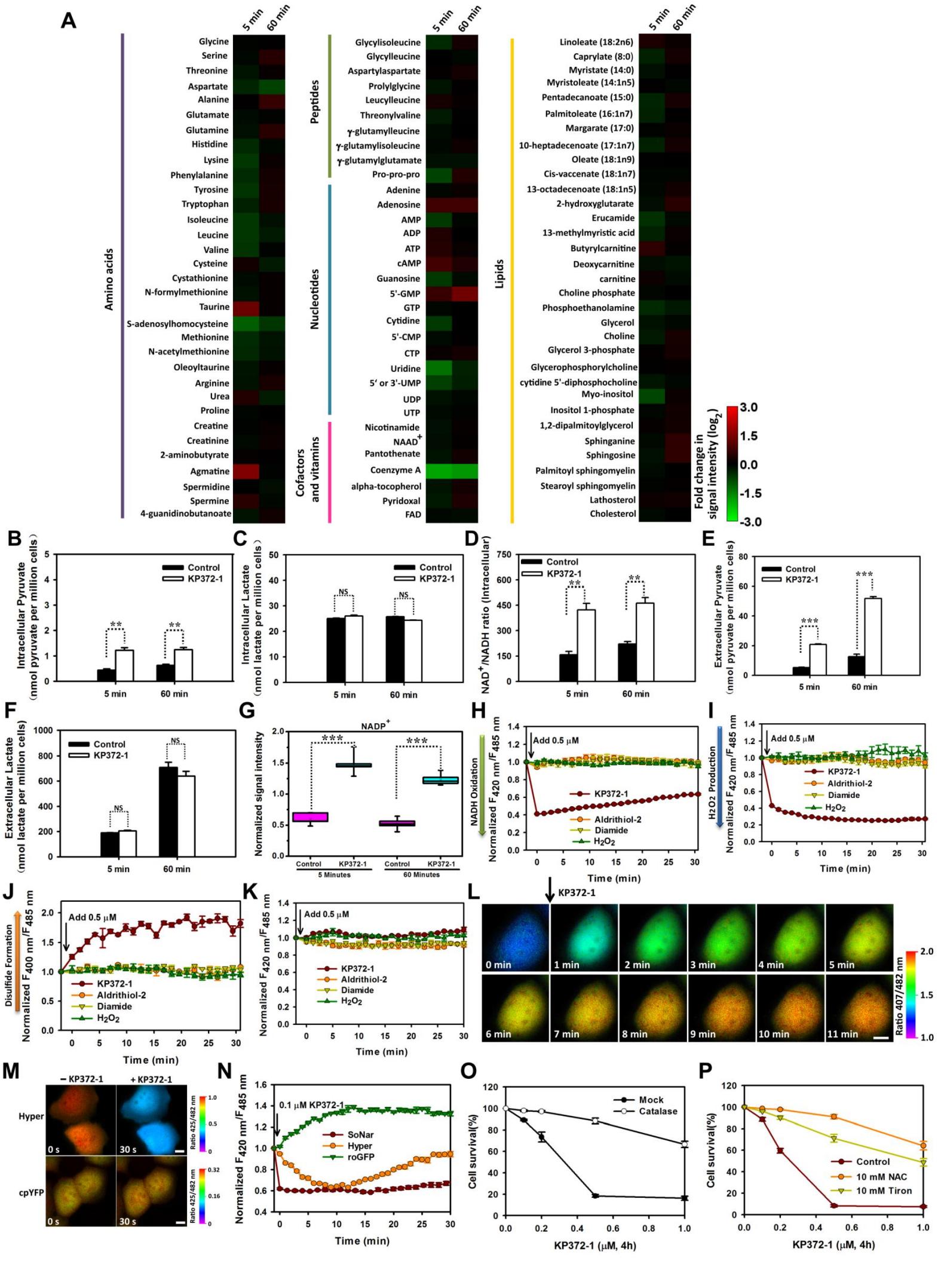
A
5 min
60 min
Amino acids
Glycine
Serine
Threonine
Aspartate
Alanine
Glutamate
Glutamine
Histidine
Lysine
Phenylalanine
Tyrosine
Tryptophan
Isoleucine
Leucine
Valine
Cysteine
Cystathionine
N-formylmethionine
Taurine
S-adenosylhomocysteine
Methionine
N-acetylmethionine
Oleoyltaurine
Arginine
Urea
Proline
Creatine
Creatinine
2-aminobutyrate
Agmatine
Spermidine
Spermine
4-guanidinobutanoate
Peptides
Glycylisoleucine
Glycylleucine
Aspartylaspartate
Prolylglycine
Leucylleucine
Threonylvaline
γ-glutamylleucine
γ-glutamylisoleucine
γ-glutamylglutamate
Pro-pro-pro
Nucleotides
Adenine
Adenosine
AMP
ADP
ATP
cAMP
Guanosine
5'-GMP
GTP
Cytidine
5'-CMP
CTP
Uridine
5' or 3'-UMP
UDP
UTP
Cofactors and vitamins
Nicotinamide
NAAD+
Pantothenate
Coenzyme A
alpha-tocopherol
Pyridoxal
FAD
Lipids
Linoleate (18:2n6)
Caprylate (8:0)
Myristate (14:0)
Myristoleate (14:1n5)
Pentadecanoate (15:0)
Palmitoleate (16:1n7)
Margarate (17:0)
10-heptadecenoate (17:1n7)
Oleate (18:1n9)
Cis-vaccenate (18:1n7)
13-octadecenoate (18:1n5)
2-hydroxyglutarate
Erucamide
13-methylmyristic acid
Butyrylcarnitine
Deoxycarnitine
carnitine
Choline phosphate
Phosphoethanolamine
Glycerol
Choline
Glycerol 3-phosphate
Glycerophosphorylcholine
cytidine 5'-diphosphocholine
Myo-inositol
Inositol 1-phosphate
1,2-dipalmitoylglycerol
Sphinganine
Sphingosine
Palmitoyl sphingomyelin
Stearoyl sphingomyelin
Lathosterol
Cholesterol
Fold change in signal intensity (log2)
3.0
1.5
0.0
-1.5
-3.0
B
Intracellular Pyruvate (nmol pyruvate per million cells)
Control
KP372-1
5 min
60 min
C
Intracellular Lactate (nmol lactate per million cells)
NS
D
NAD+/NADH ratio (Intracellular)
E
Extracellular Pyruvate (nmol pyruvate per million cells)
F
Extracellular Lactate (nmol lactate per million cells)
G
NADP+
Normalized signal intensity
5 Minutes
60 Minutes
H
Add 0.5 μM
NADH Oxidation
Normalized F420 nm/F485 nm
KP372-1
Aldrithiol-2
Diamide
H2O2
Time (min)
I
H2O2 Production
J
Disulfide Formation
Normalized F400 nm/F485 nm
K
L
KP372-1
0 min
1 min
2 min
3 min
4 min
5 min
6 min
7 min
8 min
9 min
10 min
11 min
Ratio 407/482 nm
M
– KP372-1
+ KP372-1
Hyper
cpYFP
0 s
30 s
Ratio 425/482 nm
N
0.1 μM KP372-1
SoNar
Hyper
roGFP
O
Mock
Catalase
Cell survival(%)
KP372-1 (μM, 4h)
P
Control
10 mM NAC
10 mM Tiron

Figure S6

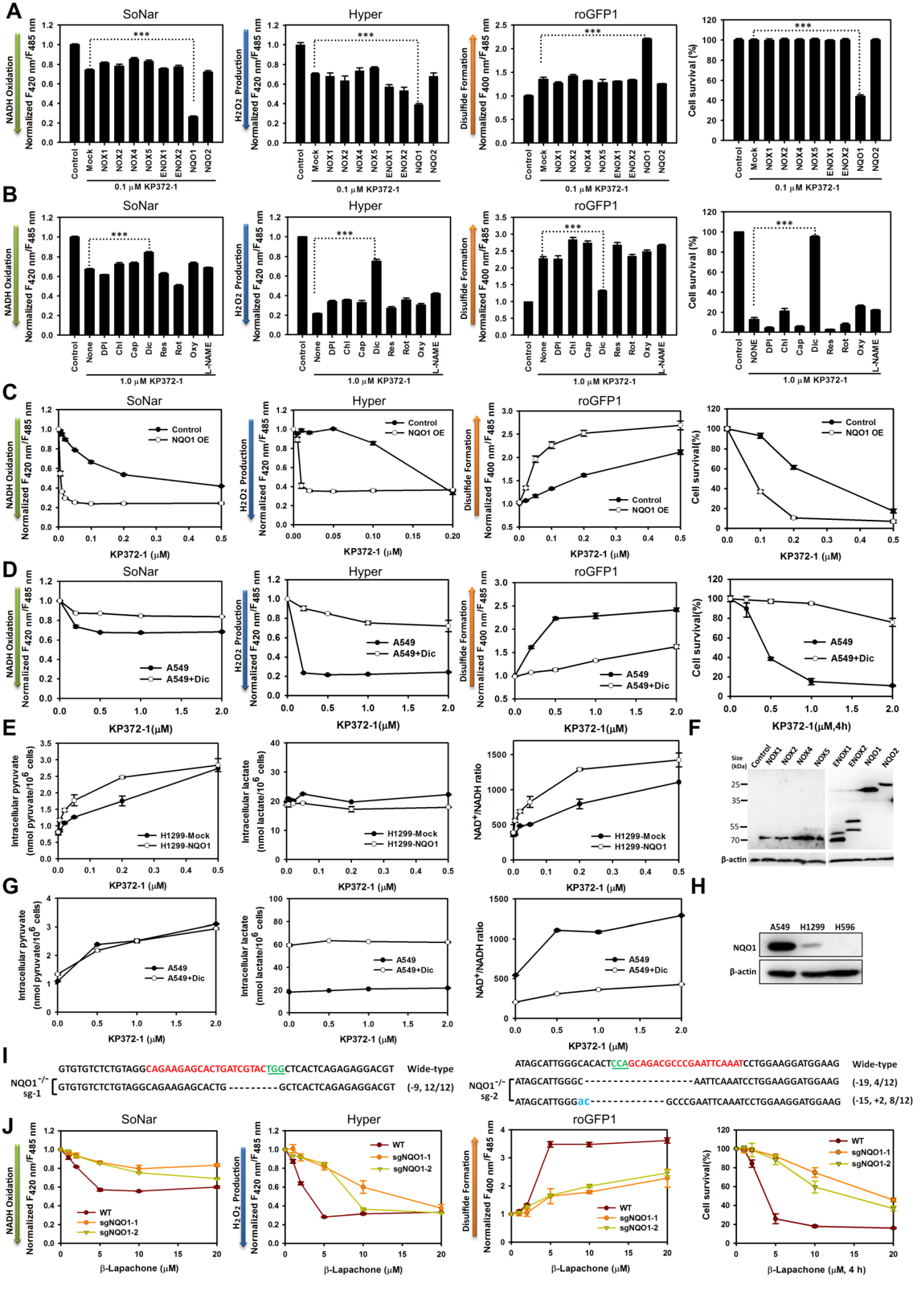
A
SoNar
Hyper
roGFP1
NADH Oxidation
H2O2 Production
Disulfide Formation
Normalized F420 nm/F485 nm
Normalized F400 nm/F485 nm
Cell survival (%)
***
Control
Mock
NOX1
NOX2
NOX4
NOX5
ENOX1
ENOX2
NQO1
NQO2
0.1 μM KP372-1
B
None
DPI
Chl
Cap
Dic
Res
Rot
Oxy
L-NAME
NONE
1.0 μM KP372-1
C
Control
NQO1 OE
KP372-1 (μM)
Cell survival(%)
D
A549
A549+Dic
KP372-1(μM)
KP372-1(μM,4h)
E
Intracellular pyruvate (nmol pyruvate/10^6 cells)
Intracellular lactate (nmol lactate/10^6 cells)
NAD+/NADH ratio
H1299-Mock
H1299-NQO1
F
Size (kDa)
25
35
55
70
β-actin
G
H
A549
H1299
H596
NQO1
β-actin
I
NQO1-/- sg-1
GTGTGTCTCTGTAGGCAGAAGAGCACTGATCGTACTGGCTCACTCAGAGAGGACGT
Wide-type
GTGTGTCTCTGTAGGCAGAAGAGCACTG---------GCTCACTCAGAGAGGACGT
(-9, 12/12)
NQO1-/- sg-2
ATAGCATTGGGCACACTCCAGCAGACGCCCGAATTCAAATCCTGGAAGGATGGAAG
Wide-type
ATAGCATTGGGC----------AATTCAAATCCTGGAAGGATGGAAG
(-19, 4/12)
ATAGCATTGGGac----------GCCCGAATTCAAATCCTGGAAGGATGGAAG
(-15, +2, 8/12)
J
WT
sgNQO1-1
sgNQO1-2
β-Lapachone (μM)
β-Lapachone (μM, 4 h)

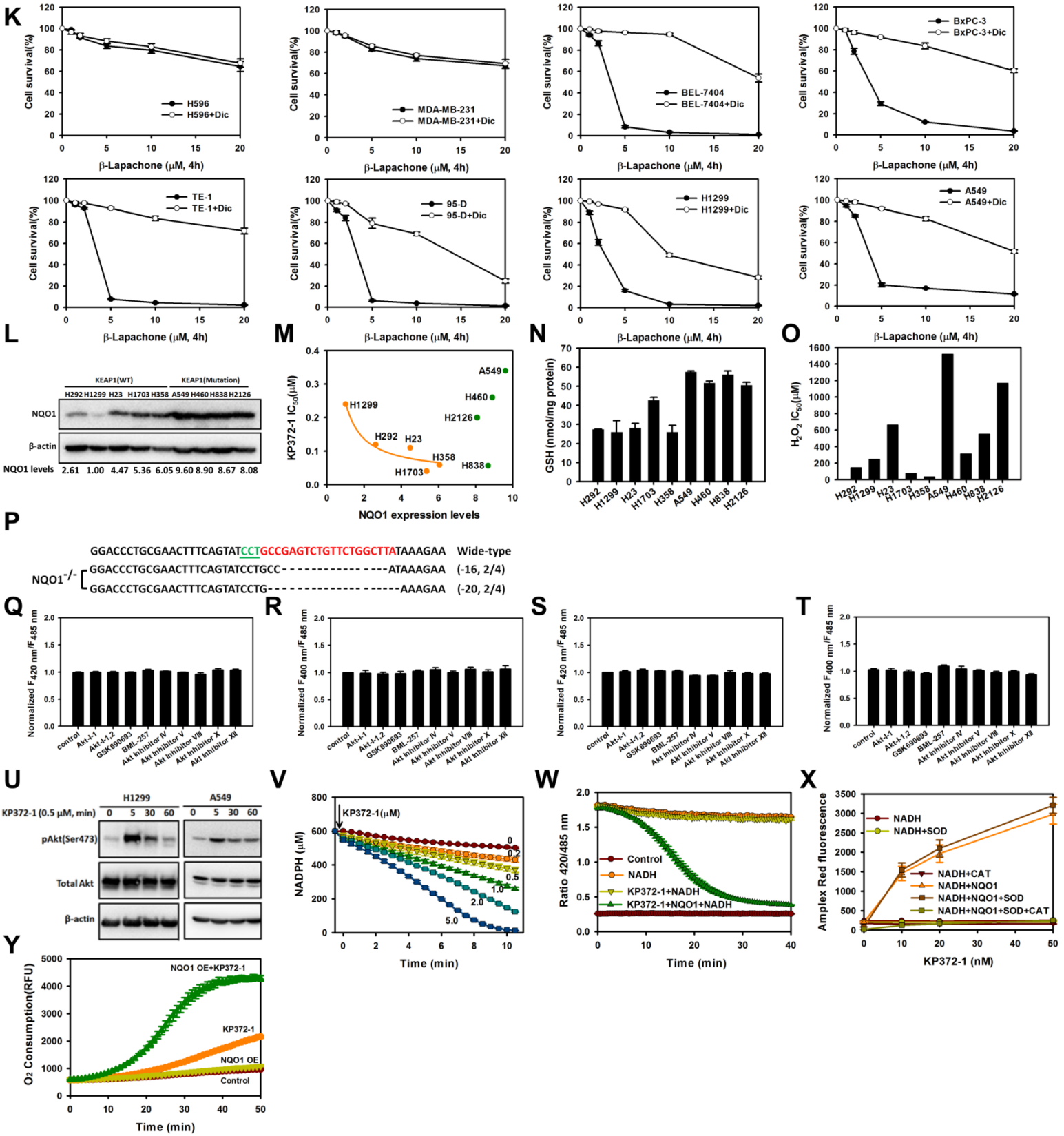
K
Cell survival(%)
β-Lapachone (μM, 4h)
H596
H596+Dic
MDA-MB-231
MDA-MB-231+Dic
BEL-7404
BEL-7404+Dic
BxPC-3
BxPC-3+Dic
TE-1
TE-1+Dic
95-D
95-D+Dic
H1299
H1299+Dic
A549
A549+Dic
L
KEAP1(WT)
KEAP1(Mutation)
H292 H1299 H23 H1703 H358 A549 H460 H838 H2126
NQO1
β-actin
NQO1 levels 2.61 1.00 4.47 5.36 6.05 9.60 8.90 8.67 8.08
M
KP372-1 IC50(μM)
NQO1 expression levels
N
GSH (nmol/mg protein)
O
H2O2 IC50(μM)
P
GGACCCTGCGAACTTTCAGTATCCTGCCGAGTCTGTTCTGGCTTATAAAGAA Wide-type
NQO1-/-
GGACCCTGCGAACTTTCAGTATCCTGC----------ATAAAGAA (-16, 2/4)
GGACCCTGCGAACTTTCAGTATCCTG----------AAAGAA (-20, 2/4)
Q
R
S
T
Normalized F420 nm/F485 nm
Normalized F400 nm/F485 nm
control
Akt-1-1
Akt-1-1,2
GSK690693
BML-257
Akt Inhibitor IV
Akt Inhibitor V
Akt Inhibitor VIII
Akt Inhibitor X
Akt Inhibitor XII
U
H1299
A549
KP372-1 (0.5 μM, min)
0 5 30 60
pAkt(Ser473)
Total Akt
β-actin
V
KP372-1(μM)
NADPH (μM)
Time (min)
W
Ratio 420/485 nm
Control
NADH
KP372-1+NADH
KP372-1+NQO1+NADH
X
Amplex Red fluorescence
NADH
NADH+SOD
NADH+CAT
NADH+NQO1
NADH+NQO1+SOD
NADH+NQO1+SOD+CAT
KP372-1 (nM)
Y
O2 Consumption(RFU)
NQO1 OE+KP372-1
KP372-1
NQO1 OE
Control
Time (min)

Table S1. Primers used for SoNar construction, truncation, and mutation, related to Figure 1.

Construction	
P1	CTAGGATCCGATGAAGGTGCCCGAGG
P2	GAT AAGCTTCTAGCCCATCATCTCCTCCCG
P3	ATACTGCAGGCTACAACAGCGACAACGTCTATATC
P4	ATAGGTACCGTTGTACTCCAGCTTGTGCCC
T-Rex-1*-Forward	ATATGGATCCATGAAGGTGCCCGAGGC
T-Rex-1*-Reverse	ATATACTAGTGCCCATCATCTCCTCCCG
T-Rex-2*-Forward	ATATGGTACCATGAAGGTGCCCGAGGC
T-Rex-2*-Reverse	ATATAAGCTTCTAGCCCATCATCTCCTCCCG
T-Rex(D2)-1*-Forward	ATATGGTACCAACCGGAAGTGGGGCCTG
T-Rex(D2)-1*-Reverse	ATATAAGCTTCTAGCCCATCATCTCCTCCCG
T-Rex(D2)-2*-Forward	ATAGGATCCGATGAACCGGAAGTGGGGCCTG
T-Rex(D2)-2*-Reverse	ATAACTAGTGCCCATCATCTCCTCCCG
H27-Forward	ATAGGTACCGGCCACCGGACCAGCAGCGAGCAG
Q24-Reverse	ATACTGCAGACTGGGCCTCCAGCTCCTCCAG
G87-Forward	ATAGGTACCGGCGGCATGGGCCGGCTGGGCAG
V86-Reverse	ATACTGCAGACACGATGCACAGGCCCCACTTCCG
R90-Forward	ATAGGTACCGGCCGGCTGGGCAGCGCCCTGGCC
G89-Reverse	ATACTGCAGAGCCCATGCCCACGATGCACAGGCC
L91-Forward	ATAGGTACCGGCCTGGGCAGCGCCCTGGCCGACTAC
R90-Reverse	ATACTGCAGACCGGCCCATGCCCACGATGCAC
S93-Forward	ATAGGTACCGGCAGCGCCCTGGCCGACTACCCCGG
G92-Reverse	ATACTGCAGAGCCCAGCCGGCCCATGCCCAC
P99-Forward	ATAGGTACCGGCCCCGGCTTCGGCGAGAGCTTC
Y98-Reverse	ATACTGCAGAGTAGTCGGCCAGGGCGCTGCC
V113-Forward	ATAGGTACCGGCGTCGACCCCGAGAAGGTGGGCC
D112-Reverse	ATACTGCAGAGTCGAAGAAGCCCCGCAGCTCG
D114-Forward	ATAGGTACCGGCGACCCCGAGAAGGTGGGCCGG
D112-Reverse	ATACTGCAGAGTCGAAGAAGCCCCGCAGCTCG
D188-Forward	ATAGGTACCGGCGACTTCCTGGCCGGCCTGACC
V187-Reverse	ATACTGCAGACACGTTCTCCACGGCCACCTCC
F189-Forward	ATAGGTACCGGCTTCCTGGCCGGCCTGACCCGG
D188-Reverse	ATACTGCAGAGTCCACGTTCTCCACGGCCACCTCC
L190-Forward	ATAGGTACCGGCCTGGCCGGCCTGACCCGGCTG
F189-Reverse	ATACTGCAGAGAAGTCCACGTTCTCCACGGCCACCTC
Truncation	
189/190-N1-Forward	GCAGGCTACAACAGCGACAACGTC

189/190-N1-Reverse	GAAGTCCACGTTCTCCACGGCCAC
189/190-N2-Forward	GGCTACAACAGCGACAACGTCTATATCATG
189/190-N3-Forward	TACAACAGCGACAACGTCTATATCATGGC
189/190-C1-Forward	CTGGCCGGCCTGACCCGGCTGAG
189/190-C1-Reverse	GGTACCGTTGTACTCCAGCTTGTGCCCCAGG
189/190-C2-Reverse	ACCGTTGTACTCCAGCTTGTGCCCCAGGATG
189/190-C3-Reverse	GTTGTACTCCAGCTTGTGCCCCAGGATGTTGC
Trex（D2）-189/190-Forward	ATGAACCGGAAGTGGGGCCTG
Trex（D2）-189/190-Reverse	CGGATCCTTATCGTCATCGTCGTAC

Note: *1, T-Rex or T-Rex(D2) locate the N terminal of cpYFP.

*2, T-Rex or T-Rex(D2) locate the C terminal of cpYFP.

Table S3. Pharmacokinetic parameters of KP372-1 in male BALB/c mice following intravenous (IV) or oral (PO) administration, related to Figure 4.

IV Group		PO Group	
Dose(mg/kg)	1	Dose(mg/kg)	5
T_{max} (hr)	-	T_{max} (hr)	0.25
C_{max} (ng/ml)	-	C_{max} (ng/ml)	1525
AUC_{last} (hr*ng/ml)	3148	AUC_{last} (hr*ng/ml)	21423
AUC_{INF} (hr*ng/ml)	4722	AUC_{INF} (hr*ng/ml)	-
$T_{1/2}$ (hr)	15.7	$T_{1/2}$ (hr)	-
V_{ss} (L/kg)	4.47	V_{ss} (L/kg)	-
Cl (L/hr/kg)	0.212	Cl (L/hr/kg)	-
MRT_{INF} (hr)	21.1	MRT_{INF} (hr)	-
F (%)*	-	F (%)*	136

*: $F=(AUC_{last\text{-}PO}*Dose_{IV})/ (AUC_{last\text{-}IV}*Dose_{PO})$

Supplemental Experimental Procedures

DNA Cloning

A synthetic gene encoding Rex from *Thermus aquaticus* (T-Rex) was designed with mammalian codon bias using Gene Designer 2.0 software(DNA 2.0)(Villalobos et al., 2006) and cloned into pRSET-B vector (Invitrogen) using the primers P1 and P2 (sequences available in Table 1). The cDNA of SoNar was generated by three separate PCRs. First, the entire coding sequences of T-Rex were amplified using several pairs of primers according to PrimersSTAR HS DNA Polymerase protocol (Takara). Second, cpYFP was amplified with P3 and P4, after which the two DNA fragments were fused by T4 DNA ligase (Fermentas). At this point, a linker, Ser-Ala-Gly, between the first part of Rex and the N terminus of cpYFP, and another linker, Gly-Gly-Cys, between the other part of Rex and C terminus of cpYFP, were incorporated. Finally, we truncated the linkers and deleted the C-terminal domain to improve affinity and specificity of the sensors by PCR. The entire coding sequence of SoNar was subcloned into pcDNA3.1/Hygro(+) vector (Invitrogen) behind a Kozak sequence for mammalian expression.

The cDNA of Enox1, Enox2, Nox1, Nox2 (CYBB), Nox4, and Nox5 gene were a kind gift from Dr. Jiahuai Han (Xiamen University), and the cDNA of NQO1 and NQO2 were purchased from Proteintech Group. To construct a mammalian cell expression vector, Enox1, Enox2, Nox1, CYBB, Nox4, Nox5, NQO1, and NQO2 genes were cloned into the pcDNA3.1/Hygro(+) vector, with 2×Flag tags added at the C-terminal end of these genes for convenient immunoassay detection. To construct an *Escherichia coli* expression vector, the NQO1 gene was constructed in-frame with the His-tag of the

pRSET-B vector. pCDNA3.1-Catalase was generated by inserting catalase cDNA into NheI/Acc651 sites of pCDNA3.1 hygro(+) vector.

For CRISPR plasmid construction, to create SpCas9 system for NQO1 gene editing, DNA oligonucleotides containing 20-nt guide sequence were phosphorylated, annealed and inserted into BbsI site in pX330 plasmid that contains the +85 chimeric RNA under the U6 promoter and a Cas9 expression cassette under the CBh promoter (Addgene ID: 42230). Constructed plasmids were sequenced to confirm the guide strand region using the primer CRISPR-R (5'- AATGGGCGGGGGTCGTTGGGCGGTC -3').

sgRNA 1Forward: 5'-CACCGCAGAAGAGCACTGATCGTAC-3'

sgRNA 1Reverse: 5'-AAACGTACGATCAGTGCTCTTCTGC-3'

sgRNA 2Forward: 5'-CACCGATTTGAATTCGGGCGTCTGC-3'

sgRNA 2Reverse: 5'-AAACGCAGACGCCCGAATTCAAATC-3'

sgRNA 3 Forward: 5'-CACCGTAAGCCAGAACAGACTCGGC-3'

sgRNA 3 Reverse: 5'-AAACGCCGAGTCTGTTCTGGCTTAC-3'

To validate the mutation sites of NQO1, the CRISPR/Cas9 target regions were amplified from the genomic DNA by PCR using primers surrounding the target region and cloned pGEM®-T Easy Vector system I(Promega), following manufacturer's instructions. Plasmid DNAs were purified and sequenced using a M13R primer (5'-AACAGCTATGACCATG -3').

PCR primer sequences for sgNQO1-1 assay:

Seq F1: 5'-AAGCCGCCCCCTCCTTTACAG-3'

Seq R1: 5'-AGAAAAAGAGAGGCTGGGGC-3'

PCR primer sequences for sgNQO1-2 assay:

Seq F2: 5’-TAGGTAGAGGGTAAGAGAGAGAC-3’

Seq R2: 5’-AGTTTAGGTCAAAGAGGCTGC-3’

PCR primer sequences for sgNQO1-3 assay:

Seq F3: 5’-TAATTAGTTCTTTGCGGATC-3’

Seq R3: 5’-AAGCACGCAAATGTCCCTGA-3’

Protein Expression and Purification

E. coli BL21 (DE3) pLys cells carrying the pRSETb-SoNar expression plasmid were grown in 10 ml LB media containing 34 μg/ml - chloramphenicol and 100 μg/ml ampicillin at 37 ^{o}C until the cultures reached about 0.4~0.6 OD. The expression of His_6-tagged proteins was induced by addition of 0.1 mM IPTG and growth continued at 18 ℃ overnight. Bacteria were then centrifuged at 4000 g for 30 min at 4 ^{o}C. The cell pellets were suspended in 1 ml 50 mM potassium phosphate buffer (Kpi buffer), pH 7.4, containing 0.5 M sodium chloride and 20 mM imidazole (Buffer A), and lysed via ultrasonication. Proteins were purified using a His MultiTrp 96-well filter plates. After washing with 2 column volumes of wash buffer (Buffer A contain 50 mM imidazole), the proteins were eluted from the resin using 50 mM Kpi buffer, pH 7.4, containing 0.5 M sodium chloride and 300 mM imidazole (Buffer B). The protein preparations were then desalted and exchanged into 100 mM HEPES buffer containing 100 mM potassium chloride (pH 7.4) before assay.

The recombinant NQO1 protein with a 6×His-tag was expressed in *E. coli* strain BL21 (DE3) plysS at 18 ^{o}C overnight in the presence of 0.1 mM IPTG and 5 μM FAD.

The cell pellet was collected by centrifugation and sonicated in buffer A containing 50 mM sodium phosphate buffer, 0.5 M NaCl, 5 µM FAD, and 10 mM imidazole, pH 7.4. The soluble cell lysate was fractionated by centrifugation. The supernatant was passed over a Ni^{2+} NTA Agarose column (GE Healthcare) and then washed thoroughly in buffer B containing 50 mM sodium phosphate buffer, 0.5 M NaCl, 5 µM FAD, and 300 mM imidazole, pH 7.4. Proteins were exchanged into 20 mM sodium phosphate buffer, 300 mM NaCl, and 5 µM FAD, pH 7.4, before assay.

Characterization of SoNar *In Vitro*

We stored the purified protein at -80 ^{o}C until experiments. Measurement of excitation and emission spectra of recombinant fluorescent sensor proteins was carried out as previously described (Zhao et al., 2011). The purified sensor protein was placed into a cuvette containing 100 mM HEPES buffer with 100 mM potassium chloride, pH 7.4. Fluorescence was measured using a Cary Eclipse spectrofluorimeter (Varian). Excitation spectra were recorded with an excitation range from 300 nm to 515 nm and an emission wavelength of 530 nm. For emission spectra, the emission range was 510-630 nm, while the excitation wavelength was 490 nm. Readings were taken every 1 nm with an integration time of 1 s, and the photomultiplier tube (PMT) voltage was set at 800 V.

For nucleotide titration, the protein was diluted in HEPES buffer (pH 7.4) to a final concentration of 0.2 µM. The fluorescence value of SoNar, in the absence of nucleotides, was measured by a filter-based Synergy 2 Multi-Mode microplate reader using 420 BP 10 nm or 485 BP 20 nm excitation and 528 BP 20 nm emission

band-pass filters (BioTek). The stock solution of nucleotides was also prepared in HEPES buffer (pH 7.4). Each assay was performed with 50 µl nucleotides and 50 µl protein in black 96-well flat bottom plate. Fluorescence intensity was read immediately after addition of nucleotide.

Cell Culture, Transfections, and Generation of Stable Cell Lines

Primary mouse renal tubular epithelial cells (RTEC), mouse embryonic fibroblast cells (MEF), mouse astrocytes, and cardiomyocytes were purchased from ALLCELLS and cultured in the recommended medium. Mouse hepatocytes were isolated and culture in complete medium 199 supplemented with 10% FBS. H1299, BEL-7404, BxPC-3, 95-D, H596, TE-1, PC-3, SPC-A-1, K-562, MKN-45, MGC80-3, CNE-1, CNE-2, Caki-2, MDA-MB-231, BEAS-2B, and QSG-7701 cells were maintained in RPMI 1640 supplemented with 10% FBS (Invitrogen). HEK293, U-87, Hela, KB, LS 174T, and MCF-7 cells were grown in DMEM (high glucose) with 10% FBS. A549 cells were cultured in F12K medium (Invitrogen) with 10% FBS. Human amniotic mesenchymal stem cells (hAMSC) were grown in alpha minimum essential medium (a-MEM) (Invitrogen) with 10% FBS. All cell lines were cultured at 37 ^{o}C in a humidified atmosphere of 95% air and 5% CO_2.

For DNA transfection, we typically used 4 µg DNA per 5×10^6 cells with 100 µl transfection buffer in 100 µl aluminum electrode cuvettes for 100 mm dish by the Nucleofector device (Amaxa, Cologne, Germany).

H1299 cells were transfected with the plasmid DNA of SoNar and cpYFP and selected in 300 µg/ml hygromycin for 2 weeks. After two weeks, the stable cells were

selected by FACSAria I (BD).

To generate NQO1 knockout cell lines, individual sgRNA constructs targeting NQO1 were transfected into A549 or H1299 cells by the Nucleofector device. After 3 days, the cells were clonally seeded into 96 well plates. A single colony with $NQO1^{-/-}$ was selected by sequencing and western blotting for further studies.

Fluorescence Microscopy

For fluorescence microscopy, H1299-SoNar-, H1299-cpYFP-, H1299-Hyper-, and H1299-roGFP1-expressing cells were plated on a 35 mm glass-bottom dish with phenol red-free growth medium. Images were acquired using a high-performance fluorescent microscopy system equipped with Nikon Eclipse Ti-E automatic microscope, monochrome cooled digital camera head DS-Qi1 Mc-U2, and the highly stable Sutter Lambda XL light source. A Plan Apo 40×0.95 NA objective was utilized. Cells were maintained at 37 ^{o}C in a humidified atmosphere using a CO_2 incubator (Tokai Hit). For dual-excitation ratio imaging, 425 BP 30 nm (407 BP 17 nm) or 482 BP 35 nm band-pass excitation filters (Semrock) and a 535 BP 40 nm emission filter altered by a Lambda 10-XL filter wheel (Shutter Instruments) were used. Images were captured using 1280×1024 format, 12 bit depth, 2×gain. Raw data were exported to ImageJ software as 12 bit TIF for analysis. The pixel-by-pixel ratio of the 482 nm excitation image by the 425 nm (407 nm) excitation image of the same cell was used to pseudocolor the images in HSB color space. Simply, the RGB value (255, 0, 255) represents the lowest ratio, and the red (255, 0, 0) represents the highest ratio, while the color brightness is proportional to the fluorescent signals in both channels.

Live-Cell Fluorescence Measurement Using Microplate Reader

Cells were harvested by trypsinization and counted by hemocytometer. Cells were washed and suspended in PBS (HyClone), and aliquots of cells were incubated at 37 ^{o}C with different compounds during the measurement. Dual-excitation ratios were obtained by a Synergy 2 Multi-Mode Microplate Reader (BioTek) with excitation filters 420 BP 10 nm (400 BP 10 nm) and 485 BP 20 nm, and emission filter 528 BP 20 nm (for both excitation wavelengths). Fluorescence values were background corrected by subtracting the intensity of the cell samples not expressing SoNar or other sensors. Unless otherwise indicated, 25 mM glucose was maintained in the buffer.

Chemical Screen and Analysis

All screened compounds were purchased from the National Compounds Resource center (China) as stock solutions in DMSO, including 180 Ascent scientific drugs, 80 kinase inhibitors, 86 SYN kinase inhibitors, 33 phosphatase inhibitors, 53 protease inhibitors, 76 nuclear receptor ligand agonists or antagonists, 202 bioactive lipid chemicals, 1280 cell signaling & neuroscience chemicals, 676 neurotransmitters, 502 natural products, 60 endocannabinoids, 446 NIH Clinical Collection compounds, 480 ICCB known bioactives chemicals, 84 orphan ligand chemicals, 68 fatty acid, 84 redox chemicals, 1440 BioBioPha chemicals, 640 FDA approved drug, 43 epigenetic chemicals, 244 Merck protein kinase inhibitors, 303 stem cell regulators, 399 InterBioScreen chemicals, and 1200 Prestwick chemicals. The majority of the compounds were arrayed in 96-well plates and diluted to 3 μM or 30 μM with PBS

containing 25 mM glucose. We then transferred 25 µl chemical solutions from 96-well plates into black 384-well flat bottom plate (Greiner Bio-one, Germany) using an 8-channel pipette and then immediately added 50 µl H1299-SoNar-expressing cell suspensions into each well using am 8-channel electronic pipette (50-1250 µl), resulting in 1 µM and 10 µM final concentrations for most compounds. Each plate contained the following control wells: 4-8 wells DMSO-only control, 2-4 wells controls with 1 mM pyruvate, and 2-4 wells controls with 5 mM oxamate. Fluorescence intensity was measured immediately. Fluorescence was assayed by a Synergy 2 Multi-Mode Microplate Reader (Bio Tek) with 420 nm or 485 nm excitation, and 528 nm emission wavelengths.

A signal 384-well plate which exhibited very low counts in all wells was excluded. Outliers that exhibited significant autofluorescence were excluded from analysis if the autofluorescence of a compound x_i is greater than or equal the value, $\left(\overline{x_{sample} - x_{blank}} \times 15\% + \bar{x}_{blank}\right)$. x_{sample} represents the fluorescence value of the compound and blank plate, and x_{blank} represents the fluorescence value of the blank plate. The raw fluorescence value (x_i) of SoNar fluorescence for each compound was transformed into a Z-score (z) to standardize the data as follows:

$$z = \frac{x_i - \mu}{\sigma}$$

μ represents the mean fluorescence value of each compound in a given plate, and σ is the standard deviation of the fluorescence value of compound in a given plate. Based on our analysis, we defined an Index (*I*) to describe the metabolic variation in the cell as follows:

$$I = \frac{(z_S - z_C)}{(z_O - z_P)}$$

z_S represents the Z-score of a given compound, z_C represents the Z-score of control, z_O represents the Z-score for treatment with oxamate, z_P represents the Z-score for treatment with pyruvate. All indices were calculated for each 384-well plate, respectively. The absolute value of *I* represents the degree of cell metabolism variation induced by this compound, whereas a *+ I* indicates a compound that increases a metabolic promoter, while a *– I* indicates a compound that decreases a metabolic promoter. The replicated measurements were averaged. The *I* value for every compound performed in our screen can be found in **Table S2**. The compound ID, CAS No, and SMILES of each compound were collected from the National Center for Drug Screening (http://www.screen.org.cn/), Shanghai, China. The canonical SMILES were generated by OpenBabel v2.3.1(O'Boyle et al., 2011) and doubled checked with PubChem compound database (http://www.ncbi.nlm.nih.gov/pccompound/). Several important physicochemical properties, including ALogP, TopoPSA, Molecular Weight (MW), and XLogP were calculated using the software PaDEL-Descriptor(Yap, 2011).

Metabolomics Analysis

The metabolomic analysis was performed by Metabolon, Inc. (Durham, NC, USA). The detailed descriptions of the platform were published previously (Evans et al., 2009; Ohta et al., 2009). Essentially, the platform used a combination of three independent methods: ultrahigh performance liquid chromatography/tandem mass spectrometry (UHLC/MS/MS^2) optimized for basic species, UHLC/MS/MS^2 optimized

for acidic species, and gas chromatography/mass spectrometry (GC/MS). 1 x 10^7 cells were extracted in 400 µl of methanol, containing recovery standards, with vigorous shaking for 2 minutes (Glen Mills Genogrinder 2000). The sample was centrifuged, the supernatant removed, and placed briefly on a TurboVap® (Zymark) to remove the organic solvent. Samples were then resuspended, divided into three equal aliquots, and prepared for the above-mentioned three instrument methods.

Measurement of Pyruvate and Lactate Production

Pyruvate and lactate production was measured using a commercially available fluorescence- based assay kit (BioVision). Cells were harvested by trypsinization and counted by hemocytometer. Cells were washed and suspended in PBS (HyClone) containing 25 mM glucose, and aliquots of cells were incubated at 37^{o}C with different compounds. For intracellular and extracellular pyruvate and lactate assay, the extracts were prepared from 7.5×10^5 cells using 500 µl ice-cold 0.25 M MPA. Extracts were centrifuged at 10,000 g. for 5 min at 4 °C, and the supernatant was neutralized with 5 M potassium carbonate. The precipitated salts were centrifuged at 10,000 g. for 5 min at 4 °C, and the supernatant was removed for assay.; For extracellular pyruvate and lactate assay, aliquots of media from each well were deproteinated as described above and assayed 5 min and 1 h later for the amount of lactate and pyruvate present.

NADPH and $NADP^+$ Levels Assay

The intracellular levels of NADPH and $NADP^+$ were measured by enzymatic cycling methods as previously described (Wagner and Scott, 1994; Zerez et al., 1987). In brief,

2×10^6 cells were lysed in 400 µL of extraction buffer (20 mM NAM, 20 mM $NaHCO_3$, 100 mM Na_2CO_3) and centrifuged at 1,200 g for 15 min. For NADPH extraction, 200 µL of the supernatant was incubated in a heating block for 30 min at 60 °C. One hundred sixty µL of NADP-cycling buffer (100 mM Tris-HCl, pH8.0; 0.5 mM thiazolylblue; 2 mM phenazine ethosulfate; 5 mM EDTA; 8.125 U/ml G6PD) was added to a 96-well plate containing 20 µL of the cell extract. After incubation for 1 min at 30 °C in the dark, 20 µL of 10 mM G6P was added to the mixture, and the changes in absorbance at 570 nm were measured every 30 sec for 10 min at 30 °C by a Synergy 2 Multi-Mode Microplate Reader. All the samples were run in triplicate. The concentration of $NADP^+$ was calculated by subtracting NADPH (heated sample) from the total of $NADP^+$ and NADPH (unheated sample).

Measurement of Total GSH and GSSG

Total glutathione (GSH + GSSG) and GSSG levels were determined as previously described (Rahman et al., 2006). All samples were run in triplicate. The rate of 2-nitro-5-thiobenzoic acid formation was calculated by the changes in absorbance at 412 nm measured every 20 sec for 10 min by a Synergy 2 Multi-Mode Microplate Reader. The GSH concentration was determined by subtracting the GSSG concentration from the total GSH concentration.

Measurement of Oxygen Consumption

Oxygen consumption was determined using the BD Oxygen Biosensor System (BD Biosciences) as described previously (Zhao et al., 2011). We added 0.55×10^6 cells to each well of the BD Oxygen Biosensor plate. Levels of oxygen consumption were

determined under baseline conditions and in the presence of different compounds. Fluorescence was recorded at 1 min intervals for 40 min by a Synergy 2 Multi-Mode Microplate Reader with excitation filter 485 BP 20 nm and emission filter 645 BP 40 nm at 37 °C.

NQO1-Dependent NAD(P)H Consumption Assay

One-tenth µg of recombinant human NQO1 was mixed with 600 µM NADH or 600 µM NADPH in 50 mM Tris-HCl, pH 7.5, and containing 0.14% bovine serum albumin. Reactions were initiated by the addition of KP372-1, and change in fluorescence at 450 nm (ex 360/40 nm, em 450/10 nm) was obtained every 30 s for 15 min.

Measurement of Superoxide Anion, Hydrogen Peroxide and Thiol Oxidation

Production of superoxide anion was measured by lucigenin-mediated chemiluminescence (Ohara et al., 1993). Fifty µl of 0.75 mM lucigenin was added to a 96-well white solid plate (Greiner Bio-one) containing 50 µl of different concentrations of KP372-1. Luminescence was measured immediately after introduction of 50 µl of assay buffer (50 mM Tris-HCl buffer, pH 7.5, containing 0.14% bovine serum albumin, 1.8 mM NADH, 0.3 µg recombinant human NQO1 with or without 90 U/ml SOD), at 46 sec intervals for 10 min by a Synergy 2 Multi-Mode Microplate Reader.

Production of hydrogen peroxide was measured by Amplex red/ horseradish peroxidase-based fluorescence (Mishin et al., 2010). Fifty µl of 150 µM Amplex red/ 0.3 U/ml horseradish peroxidase was added to a black 96-well flat bottom plate containing 50 µl of different concentration KP372-1. Fluorescence was measured

immediately after introduction of 50 µl of assay buffer (50 mM Tris-HCl buffer, pH 7.5, 30 µM NADH, 0.3 µg recombinant human NQO1 with or without 90 U/ml SOD or 900 U/ml catalase) and recorded at 1 min intervals for 10 min by a Synergy 2 Multi-Mode Microplate Reader with excitation filter 540 BP 25 nm and emission filter 590 BP 35 nm at 37 °C.

Hydrogen peroxide and thiol oxidation in live cells were measured using HyPer (Belousov et al., 2006) and roGFP1 (Dooley et al., 2004) as with SoNar described above, respectively.

Western Blot

For the Western blot analyses, cells were lysed in 1X SDS sample buffer supplemented with a protease/phosphatase inhibitor cocktail (Cell Signaling Technology). Equal amounts of total protein (10-30 µg) were separated on sodium dodecyl sulfate–polyacrylamide gel electrophoresis (SDS-PAGE), and electrotransferred onto PVDF membranes. Membranes were incubated with primary antibodies: NQO1 (Santa Cruz Biotechnologies, Santa Cruz, CA), Phospho-Akt (Ser473) , Akt, vinculin, caspase-3 (8G10) and cleaved caspase-3 (Asp175) (5A1E) (Cell Signaling Technology), β-actin and Flag (Sigma), followed by secondary antibodies conjugated to horseradish peroxidase, and addition of chemiluminescence detection mixture (Pierce, Thermo Scientific, Rockford, IL) and imaged.

Cell Viability Assay

Cell survival was determined using a Countstar automated cell counter (Inno-Alliance Biotech Inc., Wilmington, USA). For high throughput screening of cell

viability, cells were plated at a density of 3-5×10^3 cells for cancer cells, and 21x10^3 for non-cancer cells in triplicate in 96-well plates. After～20 h, cells were treated with different compounds or DMSO (0.1%). The cells were then grown for 48 h and cell viability was evaluated by the Cell Counting Kit-8 (Dojindo Laboratories, Gaithersburg, MD).

Apoptosis Assay

Translocation of phosphatidylserine to the outer plasma membrane was assessed with an Annexin V-fluorescein isothiocyanate (FITC)/propidium iodide (PI) kit (BD Pharmingen, San Diego, CA). Cells were treated with 0.5 µM KP372-1 for 24 hrs, collected and centrifuged with 1500 rpm for 5 minutes, washed once with cold PBS and then resuspended in 100 µl 1× Binding Buffer. Four µl of FITC Annexin V solution was added into cell suspension, incubated for 10 min at RT (25 °C) in the dark, then 4 µl PI and 100 µl 1× Binding Buffer added. Cells were vortexed gently and analyzed by flow cytometry within 10 min on a FACS Calibur (Becton Dickinson, San Diego, CA).

Caspase-3 Activity Assay

Caspase-3 activity was detected with the specific caspase-3 fluorogenic substrate Z-Asp-Glu-Val-Asp-7-amino-4-trifluoromethylcoumarin (Z-DEVD-AFC) (Santa Cruz Biotechnology, Dallas, TX), which liberates fluorescent AFC when cleaved by activated caspase-3. After treatment with 0.5 µM KP372-1 for 8 hours, cells were collected by scraping into cold PBS, centrifuged (at 800g for 5 minutes), and lysed in the cell lysis buffer on ice for 30 minutes. Extracts were mixed with reaction buffer containing the

Z-DEVD-AFC and incubated for 1 hour at 37 °C in the dark. The fluorescence intensity of liberated AFC was measured using a plate reader with an excitation wavelength of 400 nm and an emission wavelength of 505 nm.

Immunofluorescence

Cells were grown on coverslips and incubated with 500 nM MitoTracker Red FM (Molecular Probes) for 15 min. Cells were then fixed in 4% paraformaldehyde for 10 min, permeablized with 0.03% Triton X-100, and blocked with 5% BSA before incubation with 2% BSA containing rabbit polyclonal antibody against Bax (Abcam, ab7977) at 4°C overnight. Subsequently, the monolayers were incubated with Alexa Fluor 488-labelled goat anti-rabbit antibody (Molecular Probes) for 1 h at 37°C. Nuclei were stained with DAPI (Beyotime, China). Images were obtained at 40 × objective with a Zeiss 710 laser scanning confocal microscopy (Germany).

TUNEL Assay

The TUNEL assay was performed with the In Situ Cell Death Detection Kit (Roche). Tumors xenografts were dissected, 4% paraformaldehyde fixed, OCT-embedded, and sectioned at 10 μm thickness. Briefly, tissue sections were pre-treated with trypsin to expose DNA. The labeling reaction and detection were performed per the manufacturer's recommendation. Images were obtained at 20 × objective with Zeiss 710 laser scanning confocal microscopy (Germany).

Immunohistochemical Analysis

Paraffin-embedded tumor xenografts were sectioned, dewaxed, and subjected to antigen retrieval. Immunohistochemical staining was carried out using anti–Ki 67

(1:100; Santa Cruz Biotechnology, Dallas, TX) and anti–caspase-3 (1:50; Cell Signaling Technology, Beverly, MA) primary antibodies. Biotinylated secondary antibody and streptavidin-HRP was next applied sequentially to the slides. The color was developed with DAB mix. The slides were counterstained with hematoxylin. Images were taken via light microscope (Zeiss, Germany).

Pharmacokinetic Assay of KP372-1

Pharmacokinetic studies were performed in male BALB/c mice fasted from one night pre-dose to 4 hr post-dose. KP372-1 was formulated as 0.1 mg/ml in 0.9% NaCl (for IV) or 0.25 mg/ml in 0.9% NaCl (for PO). For intravenous administration, the solution of KP372-1 was administered as a bolus injection at 1 mg/kg dose via tail vein with 10 mL/kg volume at a slow and steady rate. For oral dosing, the test compound was administered as a uniform suspension at 5 mg/kg dose via stomach intubation using a 16-gauge oral feeding needle with a dosing volume of 20 mL/kg. Blood samples (0.11 mL) were collected from the retro-orbital sinus of a set of four mice each at t=0, 0.083, 0.25, 0.5, 1, 2, 4, 8, and 24 hr in pre-labeled microtubes containing EDTA as anticoagulant. The plasma samples were stored at -70 ℃ until bioanalysis by LC-MS/MS with lowest level of quantitation (LLOQ) = 0.636 ng/mL. Pharmacokinetic parameters (C max, T max, T ½, AUC) were calculated using a non-compartmental model with WinNonlin Ver 6.2 as statistics software (Pharsight Corporation, California, USA).

Supplemental References

Mishin, V., Gray, J.P., Heck, D.E., Laskin, D.L., and Laskin, J.D. (2010). Application of the Amplex red/horseradish peroxidase assay to measure hydrogen peroxide generation by recombinant microsomal enzymes. Free Radic Biol Med *48*, 1485-1491.

O'Boyle, N.M., Banck, M., James, C.A., Morley, C., Vandermeersch, T., and Hutchison, G.R. (2011). Open Babel: An open chemical toolbox. Journal of cheminformatics *3*, 33.

Ohara, Y., Peterson, T.E., and Harrison, D.G. (1993). Hypercholesterolemia increases endothelial superoxide anion production. J Clin Invest *91*, 2546-2551.

Rahman, I., Kode, A., and Biswas, S.K. (2006). Assay for quantitative determination of glutathione and glutathione disulfide levels using enzymatic recycling method. Nat Protoc *1*, 3159-3165.

Villalobos, A., Ness, J.E., Gustafsson, C., Minshull, J., and Govindarajan, S. (2006). Gene Designer: a synthetic biology tool for constructing artificial DNA segments. BMC Bioinformatics *7*, 285.

Wagner, T.C., and Scott, M.D. (1994). Single extraction method for the spectrophotometric quantification of oxidized and reduced pyridine nucleotides in erythrocytes. Anal Biochem *222*, 417-426.

Yap, C.W. (2011). PaDEL-descriptor: an open source software to calculate molecular descriptors and fingerprints. Journal of computational chemistry *32*, 1466-1474.

Zerez, C.R., Lee, S.J., and Tanaka, K.R. (1987). Spectrophotometric determination of oxidized and reduced pyridine nucleotides in erythrocytes using a single extraction procedure. Anal Biochem *164*, 367-373.